Available online at www.sciencedirect.com
SCIENCE DIRECT®
Journal of Photochemistry and Photobiology A: Chemistry 171 (2005) 59–67
Journal of Photochemistry and Photobiology A:Chemistry
www.elsevier.com/locate/jphotochem

Reduced mechanism for the 366 nm chlorine dioxide photodecomposition in N_2-saturated aqueous solutions

Sandra L. Quiroga[a,*], Luis J. Perissinotti[a,b]

[a] *Departamento de Química, Facultad de Ciencias Exactas y Naturales, Universidad Nacional de Mar del Plata, Funes 3350, 7600 Mar del Plata, Argentina*
[b] *Comisión de Investigaciones Científicas de la Provincia de Buenos Aires (CIC), 52610-11, 1900 La Plata, Argentina*

Received 24 June 2004; received in revised form 10 September 2004; accepted 20 September 2004
Available online 28 October 2004

Abstract

A basic reaction scheme for the integral process of chlorine dioxide (OClO) photolysis at 366 nm in N_2-saturated aqueous solution is proposed. The mechanism is supported by the initial quantum yield $\Phi^{\circ}_{366\,nm}$ determined experimentally from OClO decay rates measured by electron spin resonance (ESR), chemical analysis of the stable products in solution and numerical simulation of the OClO profiles. In the concentration range 0.5 mM ≤ [OClO] ≤ 20 mM, $\Phi^{\circ}_{366\,nm} = 0.52$ with a 95% confidence interval of 0.50–0.55. Product concentrations determined after complete photobleaching were proportional to OClO initial concentration: $[H^+] = 0.856\,[OClO]_0$; $[HClO] = (0.141 \pm 0.010)\,[OClO]_0$; $[ClO_3^-] = (0.551 \pm 0.014)\,[OClO]_0$ and $[Cl^-] = (0.251 \pm 0.015)\,[OClO]_0$. In the range of homogeneous light absorption, i.e. $[OClO]_0 \leq 1.5$ mM, OClO profiles and concentrations of the stable products in solution are well reproduced from numerical integration of the proposed mechanism. The reaction scheme requires the participation of dichlorine pentoxide (Cl_2O_5), which till now remains no isolated. However, reactions involving formation and hydrolysis of Cl_2O_5 are critical to reproduce the experimental profiles and explain the identity of the final products.

Keywords: Chlorine dioxide photolysis; Quantum yield; Dichlorine pentoxide

1. Introduction

The photolysis of chlorine dioxide (OClO) was investigated for first time in 1843 by Millon [1] and then by Popper [2] about 40 years later. Both studies focus on the products of OClO exposition to sunlight in aqueous solution and in gas phase. Quantum yields for OClO photodecomposition were determined later under monochromatic irradiation in gas or condensed phase [3–8]. In 1973, Mialocq et al. [9] studied the flash photolysis of OClO in aqueous solution and obtained the absorption spectra of Cl_2O_3 and Cl_2O_2 intermediates. By the same time, the electronic states that connect with the primary dissociation products ClO + O were identified from spectroscopic studies and the alternative products Cl + O_2 and ClOO were mentioned [10]. The production of chlorine atoms was confirmed in 1989 [11]. Because of the involvement of chlorine atoms in catalytic cycles of stratospheric ozone depletion, this result triggered a great number of publications on OClO photofragmentation in gas phase [12–17], solid matrices [18–20] and liquid solutions [21–36]. The quantum yield for Cl production was found to be phase-dependent: ≤0.04 in gas phase [13b], 1 in low-temperature matrices [18,37,38] and between 0.04 and 1 in liquid solutions [8,21,22,27]. In this context, the relaxation dynamics of OClO upon photoexcitation in different solvents has recently received attention [39–41].

In aqueous solutions, the quantum efficiencies ϕ of the primary photofragmentation steps at 355 nm were early well

* Corresponding author. Tel.: +54 223 4756167; fax: +54 223 4753150.
E-mail addresses: slquirog@mdp.edu.ar (S.L. Quiroga), 792947@copetel.com.ar (L.J. Perissinotti).

1010-6030/$ – see front matter © 2004 Elsevier B.V. All rights reserved.
doi:10.1016/j.jphotochem.2004.09.006

established [22]:

$$OClO + h\nu \rightarrow Cl + O_2, \quad \phi_1 = 0.10 \pm 0.03 \tag{1}$$

$$OClO + h\nu \rightarrow ClO + O, \quad \phi_2 = 0.90 \pm 0.05 \tag{2}$$

Two pathways are possible for reaction (1): direct dissociation and photoisomerisation to ClOO followed by peroxide dissociation. At 400 nm, 80% of Cl is produced by direct dissociation while the rest (20%) involves ClOO formation [33a,b,35a]. By comparing studies of OClO photolysis in aqueous solution under 355 and 400 nm photoexcitation, it was suggested that the mechanism of Cl production may be wavelength-dependent [36]. In addition, it was shown that the photofragments ClO + O undergo geminal recombination with gradual increase in the cage escape yield when the photolysis wavelength varies from 400 to 300 nm [29].

The ultrafast steps of OClO photochemistry begin to be clarified, however the reactions in aqueous solution that follow the primary photofragmentation channels (1) and (2) and lead to the stable products are not well described yet. Here we present a careful investigation of OClO photolysis at 366 nm in N_2-saturated aqueous solution based on OClO decay measurements and systematic analysis of the stable products. Electron spin resonance (ESR) spectroscopy allows the continuous monitoring of OClO upon irradiation as it was demonstrated in previous works [26,27]. The experimental observations are accounted by a basic mechanism which involves the formation and subsequent hydrolysis of Cl_2O_2, Cl_2O_3 and Cl_2O_5 intermediates.

2. Experimental

OClO aqueous concentrated solutions (ca. 0.1 M) were obtained by oxidising sodium chlorite ($NaClO_2$) solutions with potassium persulfate ($K_2S_2O_8$). Gaseous OClO escaping from the reaction mixture was carried by a N_2 stream, washed with aqueous solution of $NaClO_2$ and neat water, and bubbled into water at 273 K. Our determinations show that OClO is very stable in dark and frozen concentrated stock solutions.

OClO concentrations in aqueous solution were determined by 359 nm absorbance measurements in a 0.1 cm path length cuvette to minimise evaporation. The molar absorptivity determined by using standard iodometric titrimetry was found to be $1277 \pm 9\ M^{-1}\ cm^{-1}$ in good agreement with literature values [42].

N_2-saturated solutions of OClO between 0.5 and 20 mM at room temperature (≈298 K) were irradiated in a quartz cylindrical cell (internal diameter i.d. = 1.68 mm and external diameter e.d. = 3.22 mm) located within the optical microwave cavity of a Bruker X-band ESR spectrometer is as shown in Fig. 1. The height of the solution in the cell was fixed at $h = 1.1$ cm giving constant volumes of solution $V = 24.85$ μL, and ensuring the full irradiation of the sample.

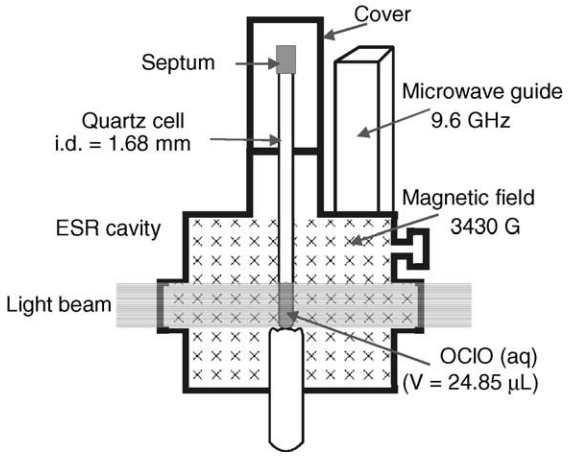

Fig. 1. Experimental set-up showing the photolysis cell in the ESR cavity.

Unbuffered solutions were used throughout in order to preserve the simplicity of the system. Aqueous OClO solutions presented pH ≈ 4 in the range of concentrations of this work. Final pHs measured after complete photobleaching were about 3. It should be stressed that OClO disproportionation and OClO reactions with other chlorine species are known to be very slow at acidic pHs [42].

The first derivative ESR signal of OClO in aqueous solution at room temperature is partially resolved in a quartet as it is expected from the spin $S = 3/2$ of both isotopes ^{35}Cl and ^{37}Cl. When the spectrum is recorded with high modulation amplitude (16 G peak-to-peak) the signal sensitivity improves by transforming the spectrum in a singlet (Fig. 2). A lineal relationship was verified between the intensity of the 16 G peak-to-peak modulated signal and OClO concentration.

A Philips HPA 400 medium-pressure metal halide lamp with iron and cobalt additives was used as source of light and 366 ± 5 nm radiation was isolated with a band-pass filter (Omega Optical).

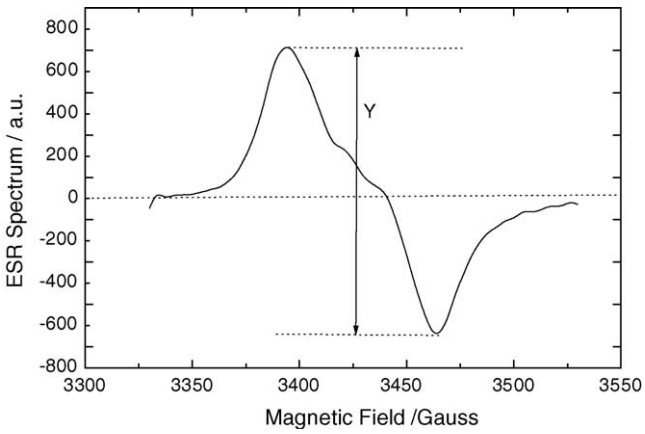

Fig. 2. First derivative X-band ESR spectrum of OClO in aqueous solution. Field modulation: 16 Gpp. The signal intensity Y is proportional to OClO concentration.

In a previous work [43], we presented a procedure to determine the absorbed photon flow $P_{a\,OClO}$ (Einstein s^{-1}) in the experimental set-up shown in Fig. 1. We found that

$$P_{a\,OClO} = FI_0h \quad (3)$$

The incident irradiance I_0 was determined in situ by using potassium ferrioxalate actinometer and varied between 1.4×10^{-9} and 2.3×10^{-9} Einstein s^{-1} cm^{-2} during the course of our experiments.

F is calculated by numerical integration [43] and depends on experimental variables: the internal and external radii of the cell, the refractive indexes of air, quartz and solution, the concentration and the molar absorption coefficient of OClO at the irradiation wavelength. Fig. 3 shows the dependence of F on OClO concentration (other parameters held constant). The plateau for high OClO concentrations indicates saturation in the light absorption. In the range of [OClO] ≤ 1.5 mM, we are able to assume homogeneous light absorption:

$$F = k_F[OClO] \quad (4)$$

From Fig. 3, $k_F = 66.35$ cm M^{-1} ($n = 5$, $r = 0.996$).

The OClO profiles obtained from ESR measurements were fitted by polynomials: $[OClO](t) = \sum_{k=0}^{n} a_k t^k$ from which the initial rate of OClO photodecomposition v_0 was readily obtained ($v_0 = a_1$).

Photolysis of the postulated reaction intermediates does not occur at the irradiation wavelength [44].

For determination of stable products in solution, photobleaching experiments of OClO in aqueous solution were carried out under stirring in 5 and 20 mL cells. Chloride, chlorate and perchlorate were determined by HPLC ion chromatography complemented with volumetric and colorimetric methods. Chloride was also analysed by argentometric titration, and a iodometric sequential method [45] was used for determination of hypochlorous acid, chlorite and chlorate.

Table 1
(A) Analytical conditions used in HPLC determinations and (B) retention times of standard ionic samples

Analytical conditions used in HPLC determinations	
Column	Shimadzu, Shim-pack IC-A1
Guard column	IC-GA1: 4.6 mm i.d. × 10 mm
Mobile phase	2.5 mM phthalic acid, 2.4 mM tris(hydroxymethyl)aminomethane (pH 4)
Flow rate	1.5 mL min^{-1}
Temperature	40 °C
Detector	Conductivity CDD-GA
Species	Retention time (min)
Retention times of standard ionic samples	
Chloride	2.78
Chlorite	2.65
Chlorate	4.33
Perchlorate	21.49

Perchlorate was analysed by the methylene blue colorimetric method [46].

Table 1A and B shows the chromatographic conditions and the retention times of standard samples of the expected products. Chloride and chlorite present similar retention times. However, chlorite is not expected as final product if chlorine/hypochlorous acid and chloride are formed. In effect, chloride is known to catalyse the chlorite disproportionation at acidic pHs while chlorite decomposition by hypochlorous acid or chloride yields variable amounts of chlorine dioxide, chloride and chlorate [45,47–50].

3. Results

3.1. Quantum yield

Initial 366 nm differential quantum yield of OClO photobleaching defined as $\Phi^{\circ}_{366\,nm} = v_0 V / P_{a\,OClO}$

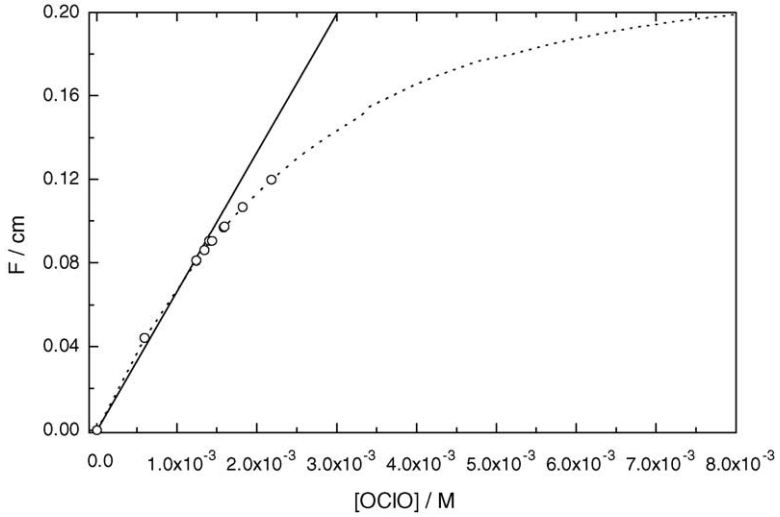

Fig. 3. Dependence of F on OClO concentration calculated as indicated in Ref. [43] (broken line), values of F for OClO diluted solutions used in a set of experiences in this work (◯), linear approximation for homogeneous absorption of light (straight line).

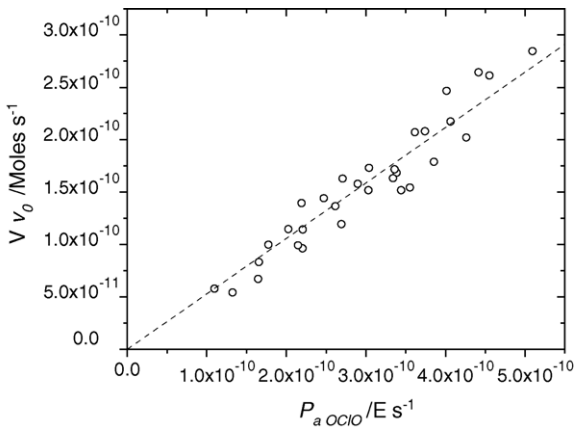

Fig. 4. Initial quantum yield for 366 nm OClO photodecomposition in aqueous N_2-saturated solutions.

was determined from the slope of Fig. 4 for $5.0 \times 10^{-4}\,M \leq [OClO]_0 \leq 2.0 \times 10^{-2}\,M$: $\Phi^{\circ}_{366\,nm} = 0.52$, with a 95% confidence interval of 0.50–0.55.

3.2. Stable products in solution

Determination of the stable photolysis products reveals the formation of chloride, hypochlorous acid and chlorate. Chlorite and perchlorate were not produced in detectable concentrations. The results from the different analysis methods were coincident.

Product concentrations determined after complete photodecomposition of OClO were proportional to OClO initial concentration: $[HClO] = (0.141 \pm 0.010)\,[OClO]_0$; $[ClO_3^-] = (0.551 \pm 0.0014)\,[OClO]_0$ and $[Cl^-] = (0.251 \pm 0.015)\,[OClO]_0$ (see Fig. 5). These findings explain the conversion of about 94% of the photolysed OClO confirming that other chlorine species are not produced in significant amounts. The difference can be attributed to losses of volatile substances like Cl_2 and OClO and errors in the determination of the substance concentrations.

Excess of chloride relative to hypochlorous acid was also analysed argentometrically after shifting the equilibrium of chlorine hydrolysis in acidic medium ($HClO + Cl^- + H^+ = Cl_2 + H_2O$) and removing Cl_2 by aspirating air through for 2 h. In this way, Cl_2/HClO interference in the argentometric titration was avoided but the result had to be corrected by the hypochlorous acid concentration to give the total chloride production.

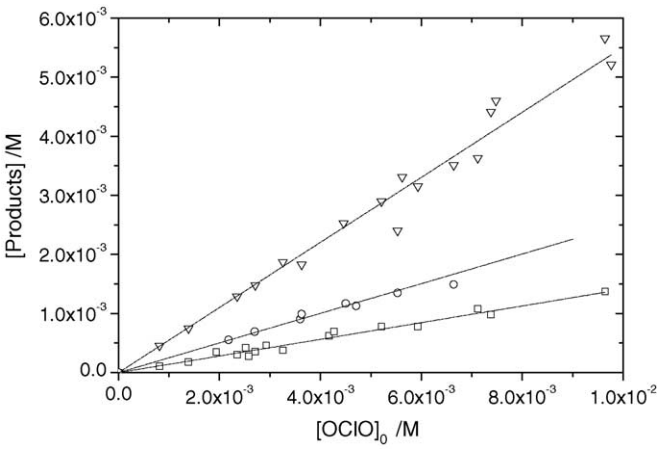

Fig. 5. Concentrations of stable products of OClO 366 nm photolysis in aqueous solution: chlorate (▽), chloride (◯) and hypochlorous acid (□). Broken lines are the linear fits of the experimental values.

4. Mechanism

4.1. Rate constants of primary photofragmentations

The rate constants of reactions (1) and (2) k_1 and k_2 are calculated by combining bibliographic data of quantum efficiencies (ϕ) [22] and cage escape yields (ξ) at 366 nm with experimental factors of irradiation (I_0) and geometry (k_F, h). Under homogeneous absorption of light, the rates of the primary events are given by the first-order equation:

$$R_i = \frac{\varphi_i P_{a\,OClO}}{V} = k_i[OClO] \quad (5)$$

with $k_i = \varphi_i k_F I_0 h$ and $\varphi_i = \xi_i \phi_i$.

At 366 nm, $\xi_1 = 1$ and $\xi_2 = 0.075$ [29], then: $\varphi_1 = 0.10 \pm 0.03$ and $\varphi_2 = 0.0675 \pm 0.0038$.

It is assumed that the irradiation wavelength only affects the cage escape yield of the photofragments ClO/O. Possible differences in the mechanism of Cl production (i.e. direct dissociation or photoisomerisation) should not modify the present analysis. Fig. 6 compares the experimental OClO profiles with the hypothetical concentration of OClO assuming that it only participates in the primary events given by reactions (1) and (2). It is apparent that secondary reactions

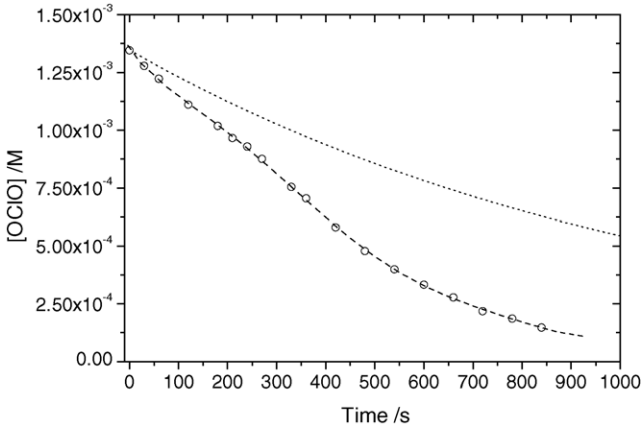

Fig. 6. Comparison between a typical experimental profile of OClO (◯) and the simulated decay (dotted line) produced from the primary photoprocesses ((1) and (2)). Initial conditions: $[OClO]_0 = 1.35 \times 10^{-3}$ M and $I_0 = 1.74 \times 10^{-9}$ Einstein s^{-1} cm^{-2}. The broken line connecting the experimental points is a polynomial regression.

make a relevant contribution to the light initiated decomposition.

4.2. Reaction scheme

The basic set of reactions that follow the primary photofragmentations and explain the experimental results involves steps (6)–(12):

$$OClO + O \rightarrow ClO_3 \quad (6)$$

$$OClO + Cl \rightarrow ClClO_2 \quad (7)$$

$$OClO + ClO \rightarrow ClOClO_2 \quad (8)$$

$$OClO + ClO_3 \rightarrow O_2ClOClO_2 \quad (9)$$

$$ClClO_2 + H_2O \rightarrow Cl^- + ClO_3^- + 2H^+ \quad (10)$$

$$ClOClO_2 + H_2O \rightarrow HClO + ClO_3^- + H^+ \quad (11)$$

$$O_2ClOClO_2 + H_2O \rightarrow 2ClO_3^- + 2H^+ \quad (12)$$

The first set of reactions (6)–(9) includes bimolecular steps producing chlorine oxide intermediates. Most of them are well characterised in gas phase [51]. Rate constants for these reactions were estimated assuming diffusion control by using the expression of Smoluchowski [52] and the Stokes–Einstein equation [53]: $k_6 = 8.8 \times 10^9\ M^{-1}\ s^{-1}$; $k_7 = 7.8 \times 10^9\ M^{-1}\ s^{-1}$; $k_8 = 7.4 \times 10^9\ M^{-1}\ s^{-1}$ and $k_9 = 7.5 \times 10^9\ M^{-1}\ s^{-1}$.

A second group of reactions (10)–(12) relates the hydrolysis of dichlorine oxides to the stable products determined in solution. Dichlorine oxides Cl_2O_n present a wide variety of isomeric structures and formal oxidation numbers [54–62] and several discrepancies on the products of their hydrolysis are observed in the literature. The species indicated in reactions (10)–(12) are produced by assuming the attack of water on the more acidic chlorine.

4.3. Simulation and sensibility analysis

The validity of the proposed mechanism was tested by numerical integration performed with a non-commercial program. The results obtained by this way indicated that the concentrations of the intermediates Cl, ClO, O, ClO_3, Cl_2O_2, Cl_2O_3 and Cl_2O_5 are smaller than 10^{-12} M, in consequence analytical resolution of the reaction scheme under steady-state approximation was addressed (see Appendix A). Both methods were coincident and reproduced adequately OClO profiles and concentrations of the stable products (see Fig. 7).

A sensitivity analysis showed that the rate constants of the bimolecular steps (6)–(9) may be reduced by a 10^3 factor without introducing changes in the concentrations of OClO and stable products. Consideration of reversal rate constants k_{-6}, k_{-7}, k_{-8} and k_{-9} for these steps did not affect the results while the steady-state condition for the intermediate holds.

Rate constants for Cl_2O_n hydrolysis species are sparse. Previous reports indicate values of 0.2 and 180 $M^{-1}\ s^{-1}$ for Cl_2O [62] and Cl_2O_2 [9], respectively. For reactions (10)–(12) we adopted $k_h = 180\ M^{-1}\ s^{-1}$ and verified that nearly the same results were obtained for $10^{-3}\ M^{-1}\ s^{-1} \leq k_h \leq 200$.

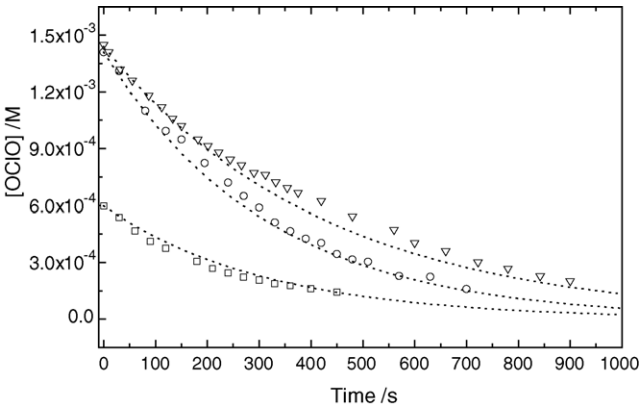

Fig. 7. Experimental and simulated (dotted line) decays of OClO 366 nm photodecomposition in aqueous solution. Initial conditions: $[OClO]_0 = 1.44 \times 10^{-3}$ M, $I_0 = 1.66 \times 10^{-9}$ Einstein $s^{-1}\ cm^{-2}$ (▽); $[OClO]_0 = 1.41 \times 10^{-3}$ M, $I_0 = 2.25 \times 10^{-9}$ Einstein $s^{-1}\ cm^{-2}$ (◯) and $[OClO]_0 = 5.97 \times 10^{-4}$ M, $I_0 = 2.25 \times 10^{-9}$ Einstein $s^{-1}\ cm^{-2}$ (□).

Although partial regeneration of OClO after turning off the light was reported in the photolysis in CCl_4 [27], we do not find evidence of OClO regeneration in aqueous solution. This result supports the hypothesis that the hydrolysis of dichlorine oxides is fast.

4.4. Perchlorate and chlorite production

Perchlorate and chlorite were not identified among the photolysis products. Earlier studies in gas phase and in carbon tetrachloride solutions by Spinks and co-workers [5,7] reported the formation of perchlorate by hydration of the photolysis products. Hydrolysis of $ClOClO_3$ and $O_2ClOClO_3$ formed in OClO photolysis in gas phase [63–65] and in CCl_4 solution produces perchlorate. However, in agreement with previous studies from other authors [8,66] we did not detect perchlorate in aqueous solution. To rationalise these findings, we included the formation of the intermediates $ClOClO_3$ and $O_2ClOClO_3$ in the reaction scheme:

$$ClO + ClO_3 \rightarrow ClOClO_3 \quad (13)$$

$$ClO_3 + ClO_3 \rightarrow O_2ClOClO_3 \quad (14)$$

and their respective hydrolysis:

$$ClOClO_3 + H_2O \rightarrow HClO + ClO_4^- + H^+ \quad (15)$$

$$O_2ClOClO_3 + H_2O \rightarrow ClO_3^- + ClO_4^- + 2H^+ \quad (16)$$

$k_{13} = 7.5 \times 10^9$ and $k_{14} = 3.7 \times 10^9\ M^{-1}\ s^{-1}$ were estimated assuming diffusion control and we adopted $k_{15} = k_{16} = k_h = 180\ M^{-1}\ s^{-1}$. Notice that reaction (9) competes with the formation of the perchlorate precursors $ClOClO_3$ and $O_2ClOClO_3$ (13) and (14). However, it is faster than steps (13) and (14) ([ClO] and $[ClO_3] \ll [OClO]$).

Table 2
Concentrations of stable products and quantum yields

	Cl^- (%)	HClO (%)	ClO_3^- (%)	ClO_4^- (%)	Φ^0
Measured	25.19	14.20	56.35	–	0.52
Steady-state approximation ($k_9 \neq 0$)	21.28	14.36	64.36	–	0.47
Simulated ($k_9 \neq 0$)	21.28	14.36	64.36	–	0.47
Simulated ($k_9 = 0$)	24.84	16.77	50.00	8.38	0.38

The concentrations of final products are expressed as percentages of $[OClO]_0$. Final concentrations of stable products and quantum yield under steady-state approximation were calculated by using Eqs. (25)–(27) and (29). The mechanism was simulated assuming that the process completes in 2000 s.

We found that the simulation of the mechanism including reactions (13)–(16) reproduced the results within experimental errors and demonstrates that concentration of perchlorate formed by these reactions is negligible ($[ClO_4^-] \approx 10^{-13}$ M). However, elimination of Cl_2O_5 formation (9) predicts the production of detectable quantities of perchlorate from steps (13)–(16) and leads to systematic deviation in OClO profiles and lower quantum yields (see Table 2 and Fig. 8).

By interrupting the irradiation during the photolysis within the ESR cavity, we observed that OClO remained constant. This result was taken as evidence that OClO does not regenerate in aqueous solution. In CCl_4, the reactive regeneration was explained by decomposition of $ClOClO_3$ [27].

Chlorite formation in secondary reactions was neglected. Additionally, it must be noted that the postulated hydrolysis mechanism only produces chlorite from species like ClOClO, OClOClO, $OClOClO_2$ or $OClOClO_3$, which are not mentioned in the current literature or have been identified only in low-temperature matrices.

4.5. Water participation in the reaction scheme

Photolysis of water does not occur at the irradiation wavelength [67]. In consequence, it only produces protons and chlorine stable products (chloride, hypochlorous acid and chlorate) by reaction with the dichlorine oxide intermediates.

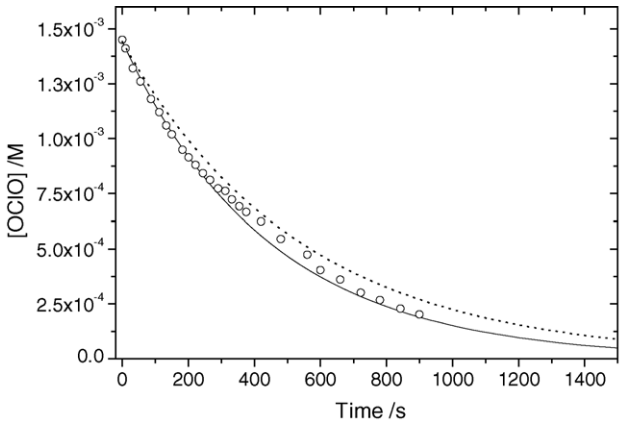

Fig. 8. Effect of excluding Cl_2O_5 formation in OClO profile. Simulation of the proposed mechanism with $k_9 = 0$ (broken line) and $k_9 = 7.5 \times 10^9\ M^{-1}\ s^{-1}$ (solid line). The open circles are the experimental points for $[OClO]_0 = 1.41 \times 10^{-3}$ M and $I_0 = 2.25 \times 10^{-9}$ Einstein $s^{-1}\ cm^{-2}$.

There are not references to reactions of the primary photofragments (O, Cl and ClO) with water except for Cl which undergoes reactions (17)–(24) [68].

$$Cl + H_2O \rightarrow HClO^- + H^+, \quad k_{17} = 4.5 \times 10^3\ M^{-1}\ s^{-1}, \quad k_{-17} = 2.1 \times 10^{10}\ M^{-1}\ s^{-1} \tag{17}$$

$$HClO^- \rightarrow Cl^- + OH, \quad k_{18} = 6.1 \times 10^9\ M^{-1}\ s^{-1}, \quad k_{-18} = 4.3 \times 10^9\ M^{-1}\ s^{-1} \tag{18}$$

$$Cl + Cl^- \rightarrow Cl_2^-, \quad k_{19} = 8.5 \times 10^9\ M^{-1}\ s^{-1}, \quad k_{-19} = 6.0 \times 10^4\ s^{-1} \tag{19}$$

$$Cl_2^- + H_2O \rightarrow HClO^- + Cl^- + H^+, \quad k_{20} = 1.3 \times 10^3\ s^{-1} \tag{20}$$

$$OClO + OH \rightarrow ClO_3^- + H^+, \quad k_{21} = 2.6 \times 10^9\ M^{-1}\ s^{-1} \tag{21}$$

$$OClO + OH \rightarrow HClO + O_2, \quad k_{22} = 1.4 \times 10^9\ M^{-1}\ s^{-1} \tag{22}$$

$$HClO + OH \rightarrow ClO + H_2O, \quad k_{23} = 1.4 \times 10^8\ M^{-1}\ s^{-1} \tag{23}$$

$$Cl_2^- + OClO \rightarrow ClClO_2 + Cl^-, \quad k_{24} = 1.0 \times 10^9\ M^{-1}\ s^{-1} \tag{24}$$

We probed that OClO profiles and concentrations of the stable products in solution were not affected by including steps (17)–(24) in the reaction scheme.

4.6. Expressions for product concentrations and quantum yield

Ratios of product P_j formation rate relative to OClO decomposition rate $\alpha_j = -d[P_j]/d[OClO]$ were obtained by solving the reaction scheme under steady-state approximation (see Appendix A):

$$\alpha_{Cl^-} = \frac{k_1}{2k_1 + 4k_2} = \frac{\varphi_1}{2\varphi_1 + 4\varphi_2} \tag{25}$$

$$\alpha_{HClO} = \frac{k_2}{2k_1 + 4k_2} = \frac{\varphi_2}{2\varphi_1 + 4\varphi_2} \tag{26}$$

$$\alpha_{ClO_3^-} = \frac{k_1 + 3k_2}{2k_1 + 4k_2} = \frac{\varphi_1 + 3\varphi_2}{2\varphi_1 + 4\varphi_2} \quad (27)$$

These equations show that the product concentrations are directly proportional to [OClO] in agreement with the experimental determinations.

The mechanism also predicts a linear variation of $[H^+]$ with the concentration of OClO photolysed:

$$a_{H^+} = \frac{2k_1 + 3k_2}{2k_1 + 4k_2} = \frac{2\varphi_1 + 3\varphi_2}{2\varphi_1 + 4\varphi_2} \quad (28)$$

By replacing v_0 with the analytical expression for d[OClO]/dt (see Appendix A), the initial quantum yield $\Phi^\circ_{366\,nm} = v_0 V / P_{a\,OClO}$ results:

$$\Phi^\circ_{366\,nm} = 2\varphi_1 + 4\varphi_2 \quad (29)$$

Notice that the expressions (25)–(29) are exclusively dependent on the effective quantum efficiencies (φ) and they give values close to the experimental results (see Table 2).

5. Conclusions

Experimental results determined in OClO photolysis at 366 nm in N_2-saturated aqueous solutions can be explained by a simple reaction scheme which includes the current knowledge about the primary photoprocesses and the structure of dichlorine oxide intermediates.

The proposed mechanism is composed by only nine reactions: the two primary photoprocesses, four bimolecular steps of OClO with the primary photofragments or the radical ClO_3 producing chlorine oxide intermediates, and three hydrolysis reactions leading to the stable products in solution. However, it reproduces the OClO profiles and accounts quantitatively for the relative concentrations of the stable products, chlorate, chloride and hypochlorous acid. Notice that all the hydrolysis reactions produce chlorate which is the major product while chloride concentration relative to hypochlorous acid concentration is in the ratio of φ_1/φ_2 within the experimental error.

Qualitative scheme is presented in Fig. 9 and resumed by reaction (30) from which approximated values of quantum yield and product concentrations relative to OClO consumption can be derived:

$$22OClO + 11H_2O + 44h\nu \rightarrow 14ClO_3^- + 5Cl^- + 3HClO + 5O_2 + 19H^+ \quad (30)$$

Then: $\Phi = 22/44 = 0.50$, $\alpha_{ClO_3^-} = 14/22 = 0.636$, $\alpha_{Cl^-} = 5/22 = 0.227$ and $\alpha_{HClO} = 3/22 = 0.136$.

As it was indicated in Section 4.4, Cl_2O_5 participation is responsible for the absence of perchlorate among the photolysis products. Cl_2O_5 was not isolated up till now but a theoretical study [56] predicts the stability of the structure proposed in this work which produces chlorate by hydrolysis. In aqueous solution, the hydrolysis would prevent the Cl_2O_5 decomposition producing chlorate instead of perchlorate while in gas phase or in CCl_4 solution we suggest that Cl_2O_5, if formed, would be readily decomposed. In the last case, $k_h = 0$ favours the formation of the perchlorate precursors.

O_2 formed in reaction (1) does not produce appreciable effect. Work in O_2-saturated solutions will be presented in a separate paper.

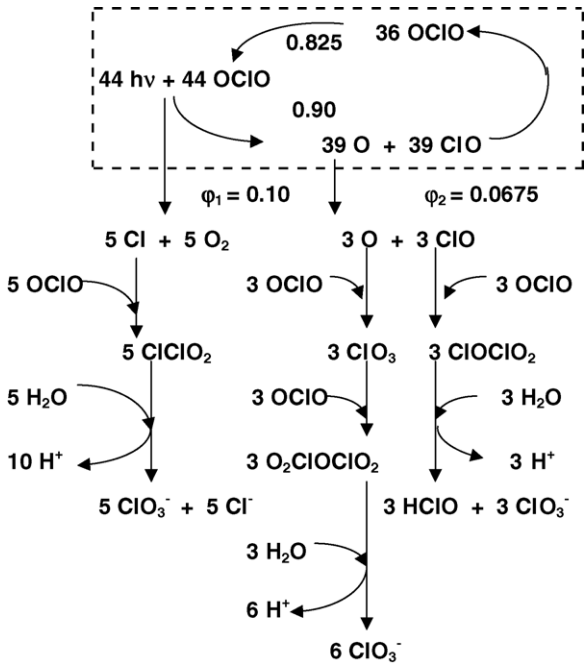

Fig. 9. Schematic representation of the mechanism proposed for 366 nm OClO photodecomposition in N_2-saturated aqueous solution.

Acknowledgments

The authors acknowledge financial support from the University of Mar del Plata and thank to G. Duda from FIDEX SA for technical assistance in the HPLC analysis of the photodecomposition products.

Appendix A. Steady-state approximation

The complete reaction scheme including steps (1), (2), (6)–(16) and the reversal of the bimolecular reactions (6)–(9), (13), (14) was solved under steady-state approximation.

$$\frac{d[OClO]}{dt} = -(k_1 + k_2 + k_6[O] + k_7[Cl] + k_8[ClO] + k_9[ClO_3])[OClO] + k_{-6}[ClO_3] + k_{-7}[Cl_2O_2] + k_{-8}[Cl_2O_3] + k_{-9}[Cl_2O_5] \quad (A.1)$$

The steady-state differential equations for the nine reaction intermediates were solved with Derive [69] mathematical assistant program.

By replacing the intermediate concentrations in Eq. (A.1):

$$\frac{d[OClO]}{dt} = -(2k_1 + 4k_2)[OClO] + 2\frac{k_{13}k_h}{k_h + k_{-13}} \times [ClO][ClO_3] + 2\frac{k_{14}k_h}{k_h + k_{-14}}[ClO_3]^2 \quad (A.2)$$

In the same way, reaction rates corresponding to the formation of the final products result:

$$\frac{d[Cl^-]}{dt} = k_1[OClO] \quad (A.3)$$

$$\frac{d[HClO]}{dt} = k_2[OClO] \quad (A.4)$$

$$\frac{d[ClO_3{}^-]}{dt} = (k_1 + 3k_2)[OClO] - 3\frac{k_{13}k_h}{k_h + k_{-13}} \times [ClO]\,[ClO_3] - 3\frac{k_{14}k_h}{k_h + k_{-14}}[ClO_3]^2 \quad (A.5)$$

$$\frac{d[ClO_4{}^-]}{dt} = \frac{k_{13}k_h}{k_h + k_{-13}}[ClO][ClO_3] + \frac{k_{14}k_h}{k_h + k_{-14}}[ClO_3]^2 \quad (A.6)$$

It can be demonstrated that the terms containing products of intermediate species concentrations are numerically negligible. Then, negligible formation of perchlorate is predicted by Eq. (A.6). In the same way, by eliminating the non-lineal terms in Eq. (A.2) it results a first-order equation which only depends on the rate constants of the primary photoprocesses:

$$\frac{d[OClO]}{dt} = -(2k_1 + 4k_2)[OClO] \quad (A.7)$$

References

[1] M. Millon, Ann. Chim. Phys. 7 (1843) 298–339.
[2] A. Popper, Ann. Chem. 227 (1885) 161–180.
[3] (a) E.J. Bowen, J. Am. Chem. Soc. 123 (1923) 1199–1206;
(b) H. Booth, E.J. Bowen, J. Am. Chem. Soc. 127 (1925) 510–513.
[4] J.W.T. Spinks, J. Am. Chem. Soc. 54 (1932) 1689–1690.
[5] J.W.T. Spinks, J.M. Porter, J. Am. Chem. Soc. 56 (1934) 264–270.
[6] Y. Nagai, C.F. Goodeve, Trans. Faraday Soc. 27 (1931) 508–513.
[7] (a) J.W.T. Spinks, H. Taube, J. Am. Chem. Soc. 59 (1937) 1155–1156;
(b) J.W.T. Spinks, H. Taube, Can. J. Res. 15 (1937) 499–524.
[8] E.J. Bowen, W.M. Cheung, J. Chem. Soc. 127 (1932) 1200–1207.
[9] J.C. Mialocq, F. Barat, L. Gilles, B. Hickel, B. Lesigne, J. Phys. Chem. 77 (1973) 742–749.
[10] P.A. Mc Donald, K.K. Innes, Chem. Phys. Lett. 59 (1978) 562–566.
[11] V. Vaida, S. Solomon, E.C. Richard, E. Rühl, A. Jefferson, Nature 342 (1989) 405–408.
[12] (a) E. Bishenden, J. Haddock, J. Donaldson, J. Phys. Chem. 95 (1991) 2113–2115;
(b) E. Bishenden, J. Donaldson, J. Chem. Phys. 99 (1993) 3129–3132;
(c) E. Bishenden, J. Donaldson, J. Chem. Phys. 101 (1994) 9565–9572.
[13] (a) J.F. Davis, Y.T. Lee, J. Phys. Chem. 96 (1992) 5681–5684;
(b) H.F. Davis, Y.T. Lee, J. Chem. Phys. 105 (1996) 8142–8163.
[14] R. Flesch, E. Rühl, K. Hottmann, H. Baumgärtel, J. Phys. Chem. 97 (1993) 837–844.
[15] T. Baumert, J.L. Herek, A.H. Zewall, J. Chem. Phys. 99 (1993) 4430–4440.
[16] K.A. Peterson, H. Werner, J. Chem. Phys. 105 (1996) 9823–9832.
[17] (a) M. Roth, C. Maul, K. Gericke, J. Chem. Phys. 107 (1997) 10582–10591;
(b) R.F. Delmdahl, S. Ulrich, K. Gericke, J. Phys. Chem. A 102 (1998) 7680–7685;
(c) R.F. Delmdahl, S. Welcker, K. Gericke, Ber. Bunsenges Phys. Chem. 102 (1998) 244–248.
[18] C.J. Pursell, J. Conyers, P. Alapat, R. Parveen, J. Phys. Chem. 99 (1995) 10433–10437.
[19] C.J. Pursell, J. Conyers, C. Denison, J. Phys. Chem. 100 (1996) 15450–15453.
[20] J.D. Graham, J.T. Roberts, L.D. Anderson, V.H. Grassian, J. Phys. Chem. 100 (1996) 19551–19558.
[21] R.C. Dunn, E.C. Richard, V. Vaida, J.D. Simon, J. Phys. Chem. 95 (1991) 6060–6063.
[22] (a) R.C. Dunn, B.N. Flanders, V. Vaida, J.D. Simon, Spectrochim. Acta, Part A 48 (1992) 1293–1301;
(b) R.C. Dunn, J.D. Simon, J. Am. Chem. Soc. 114 (1992) 4856–4860;
(c) R.C. Dunn, J.L. Anderson, C.S. Foote, J.D. Simon, J. Am. Chem. Soc. 115 (1993) 5307.
[23] V. Vaida, K. Goudjil, J.D. Simon, B.N. Flanders, J. Mol. Liq. 61 (1994) 133–152.
[24] V. Vaida, J.D. Simon, Science 268 (1995) 1443–1448.
[25] R.C. Dunn, B.N. Flanders, J.D. Simon, J. Phys. Chem. 99 (1995) 7360–7370.
[26] M.S. Churio, M.A. Brusa, L.J. Perissinotti, E. Ghibaudi, M.E.J. Coronel, A.J. Colussi, Chem. Phys. Lett. 232 (1995) 237–241.
[27] M.A. Brusa, L.J. Perissinotti, M.S. Churio, A.J. Colussi, J. Photochem. Photobiol. A 101 (1996) 105–111.
[28] Y.J. Chang, J.D. Simon, J. Phys. Chem. 100 (1996) 6406–6411.
[29] J. Torgersen, P.U. Jepsen, C.L. Tomsen, J.Aa. Poulsen, J.R. Byberg, S.R. Keiding, J. Phys. Chem. A 101 (1997) 3317–3323.
[30] M.J. Philpott, S. Charalambous, P.J. Reid, J. Chem. Phys. Lett. 281 (1997) 1–9.
[31] (a) A.P. Esposito, C.E. Foster, R.A. Beckman, P.J. Reid, J. Phys. Chem. A 101 (1997) 5309–5319;
(b) P.J. Reid, A.P. Esposito, C.E. Foster, R.A. Beckman, J. Chem. Phys. 167 (1997) 8262–8274;
(c) C.E. Foster, P.J. Reid, J. Phys. Chem. A 102 (1998) 3514–3523;
(d) S.C. Hayes, M.P. Philipott, P.J. Reid, J. Chem. Phys. 109 (1998) 2596–2599;
(e) S.C. Hayes, M.P. Philipott, S.G. Mayer, P.J. Reid, J. Phys. Chem. A 103 (1999) 5534–5546.
[32] J. Torgersen, C.L. Tomsen, J.Aa. Poulsen, S.R. Keiding, J. Phys. Chem. A 102 (1998) 4186–4191.
[33] (a) C.L. Tomsen, P.J. Reid, S.R. Keiding, J. Am. Chem. Soc. 122 (2000) 12795–12801;
(b) C.L. Tomsen, M.P. Philipott, S.C. Hayes, P.J. Reid, J. Chem. Phys. 112 (2000) 505–508;
(c) S.C. Hayes, C.L. Tomsen, P.J. Reid, J. Chem. Phys. 115 (2001) 11228–11238.
[34] (a) S.C. Hayes, C.C. Cooksey, P.M. Wallace, P.J. Reid, J. Phys. Chem. A 105 (2001) 9819–9826;
(b) C.E. Foster, B.P. Barham, P.J. Reid, J. Chem. Phys. 114 (2001) 8492–8504.

[35] (a) P.J. Reid, Acc. Chem. Res. 34 (2001) 691–698;
(b) P.J. Reid, J. Phys. Chem. A 106 (2002) 1473–1474.
[36] P.M. Wallace, J.C. Bolinger, S.C. Hayes, P.J. Reid, J. Chem. Phys. 118 (2003) 1883–1890.
[37] A. Arkell, I. Schwager, J. Am. Chem. Soc. 89 (1967) 5999–6006.
[38] H.S.P. Muller, H. Willner, J. Phys. Chem. 97 (1993) 10589–10598.
[39] H. Fidder, F. Tachirschwitz, O.P. Dühr, E.T.J. Nibbering, J. Chem. Phys. 114 (2001) 6781–6794.
[40] I. Chorny, J. Vieceli, I. Benjamin, J. Chem. Phys. 116 (2002) 8904–8911;
I. Chorny, J. Vieceli, I. Benjamin, J. Chem. Phys. 116 (2002) 8930–8937.
[41] C. Brooksby, O.V. Prezhdo, P.J. Reid, J. Chem. Phys. 118 (2003) 4563–4572;
C. Brooksby, O.V. Prezhdo, P.J. Reid, J. Chem. Phys. 119 (2003) 9111–9120.
[42] R.G. Kieffer, G. Gordon, Inorg. Chem. 7 (1968) 235–244.
[43] S.L. Quiroga, M.S. Churio, L.J. Perissinotti, Appl. Magn. Reson. 22 (2002) 115–131.
[44] R.P. Wayne, G. Poulet, P. Biggs, J.P. Burrows, R.A. Cox, P.J. Crutzen, G.D. Hayman, M.E. Jenkin, G. Le Bras, G.K. Moortgat, U. Platt, R.N. Schindler, Atmos. Environ. 29 (1995) 2677–2881.
[45] G. Gordon, W.J. Cooper, R.G. Rice, G.E. Pacey, Research Report: Disinfectant Residual Measurement Methods, AWWA, USA, 1987.
[46] D.F. Boltz, W.J. Holland, J.A. Howell, Colorimetric determination of nonmetals, in: Chemical Analysis, vol. 8, Wiley, USA, 1978, p. 100.
[47] Z. Jia, D.W. Margerum, J.S. Francisco, Inorg. Chem. 39 (2000) 2614–2620.
[48] R.G. Kieffer, G. Gordon, Inorg. Chem. 7 (1968) 235–244.
[49] F. Emmenegger, G. Gordon, Inorg. Chem. 6 (1967) 633–634.
[50] H. Taube, H. Dodgen, J. Am. Chem. Soc. 71 (1949) 3330–3336.
[51] Chemical Kinetics and Photochemical Data for Use in Stratospheric Modeling: Evaluation Number 9, NASA, 1990.
[52] J.W. Moore, R.G. Pearson, Kinetics and Mechanism, Wiley, USA, 1981, pp. 237–240.
[53] J.H. Espenson, Chemical Kinetics and Reaction Mechanisms, McGraw-Hill, USA, 1995, pp. 199–201.
[54] B.T. Luke, J. Mol. Struct. (TEOCHEM) 332 (1995) 283–289.
[55] H.S.P. Müller, E.A. Cohen, J. Phys. Chem. A 101 (1997) 3049–3051.
[56] A.J. Colussi, M.A. Grela, Int. J. Chem. Kinet. 30 (1998) 41–45.
[57] D. Christen, H.G. Mack, H.S.P. Müller, J. Mol. Struct. (TEOCHEM) 509 (1999) 137–151.
[58] (a) C.J. Schack, D. Pilipovich, Inorg. Chem. 9 (1970) 1387–1390;
(b) K.O. Christe, C.J. Schack, E.C. Curtis, Inorg. Chem. 10 (1971) 1589–1593.
[59] M.I. Lopez, J.E. Sicre, J. Phys. Chem. 92 (1988) 563–564.
[60] R.R. Friedl, M. Birk, J.J. Oh, E.A. Cohen, J. Mol. Spectrosc. 170 (1995) 383–396.
[61] K.H. Kim, Y.K. Han, Y.S. Lee, J. Mol. Struct. (TEOCHEM) 460 (1999) 19–25.
[62] M.W. Beach, D.W. Margerum, Inorg. Chem. 29 (1990) 1225.
[63] A.J. Schell-Sorokin, D.S. Bethune, J.R. Lankard, M.M.T. Loy, P.P. Sorokin, J. Phys. Chem. 86 (1982) 4653–4655.
[64] F. Zabel, Ver. Bunsenges. Phys. Chem. 95 (1991) 893–900.
[65] A.J. Colussi, J. Am. Chem. Soc. 94 (1990) 8922–8926.
[66] H. Cosson, W.R. Ernst, Ind. Eng. Chem. Res. 33 (1994) 1468–1475.
[67] J.G. Calvert, J.N. Pitts, Photochemistry, Wiley, USA, 1966, p. 200.
[68] (a) W.J. McElroy, J. Phys. Chem. 94 (1990) 2435–2441;
(b) H.W. Jacobi, H. Herrmann, R. Zellner, Ver. Bunsenges. Phys. Chem. 101 (1997) 1909–1913;
(c) G.V. Buxton, M. Bydder, G.A. Salmon, J. Chem. Soc., Faraday Trans. 94 (1998) 653–657;
(d) Z. Zuo, Y. Katsumura, K. Ueda, K. Ishigure, Chem. Soc. Faraday Trans. 93 (1997) 1885–1891.
[69] Derive, Version 5.00, Texas Instruments, 1988–2000.